PHYSICAL REVIEW VOLUME 121, NUMBER 2 JANUARY 15, 1961

Formation of F Centers in KCl by X Rays*†

P. V. Mitchell,‡ D. A. Wiegand, and R. Smoluchowski§
Carnegie Institute of Technology, Pittsburgh, Pennsylvania

(Received June 23, 1960; revised manuscript received September 21, 1960)

Measurements have been made of the growth of the F band in undeformed, deformed, and heat-treated KCl crystals at room temperature using 140-kvp x-ray irradiation. The growth curves were analyzed in terms of the initial concentration of negative-ion vacancies in the lattice before irradiation, rate of formation of new vacancies, rate of electron capture by the initial and by the new vacancies, and bleaching constants. These parameters were studied as a function of the intensity of irradiation. It appears that the new vacancies are generated at a rate proportional to the square of the intensity of irradiation and inversely proportional to the dislocation density. Deformation increases the concentration of initial vacancies near dislocations, while heat treatment increases the concentration of initial vacancies dispersed in the volume of the crystal. Since neither the jog mechanism nor the Varley mechanism can account for the observations, a new model is proposed which accounts for all the observed phenomena.

I. INTRODUCTION

It is believed that F centers are formed in alkali halides by x rays by two distinct processes. In one of them negative-ion vacancies initially present in the crystal may trap electrons liberated by x rays. In the other one new vacancies are generated[1,2] and these in turn may trap electrons and form additional F centers. In a heavily irradiated crystal only a small fraction of the F centers can be attributed to the initial vacancies.

The usual assumption that the initial vacancies and those generated by irradiation are indistinguishable from each other leads to a rate of coloration of a crystal given by

$$df/dt=b(n_0+at-f)\quad (f=0 \text{ at } t=0)$$

which gives

$$f=\left(n_0-\frac{a}{b}\right)(1-e^{-bt})+at,$$

where f is the density of centers, a is the rate of generation of new vacancies, and b is a rate constant for capture of electrons. Mador *et al.*[3] and later Gordon and Nowick[4] have found that there are indeed two distinct stages in the growth curves of F centers in the alkali halides: an early rapid rise followed by a slow linear increase. This is qualitatively in agreement with the shape predicted by the above equation. More recent work[5–8] shows, however, that this relatively simple model and equation are not always applicable, since some growth curves have an inflection point as shown in Fig. 1. It has been shown in our earlier paper[7] that in order to fit a theoretical curve to the experimental data for KCl one has to make the assumption that the new and the initial vacancies behave in many ways differently. The main result of this analysis is the quadratic dependence on x-ray intensity of the rate constant for the generation of new vacancies and the big difference between the cross sections for electron capture by the initial and by the new vacancies. The present paper is an extension and a more detailed development of this analysis, its application to irradiation of as-cleaved, of deformed, and of heat-treated crystals, and a quantitative discussion of its consequences. As before, KCl was chosen as the subject of investigation because of the wealth of data already available on this system.

II. THEORETICAL CONSIDERATIONS

A. Growth of F Centers

A typical room temperature growth curve of the optical density of the F band shows an early rapid rise to between 10^{16} and 10^{17} centers/cm^3, followed by an approximately linear, relatively slow rise until saturation at about 10^{18}–10^{19} centers/cm^3. The early period is the most efficient, requiring only a few hundred electron volts per center, while the linear part requires several thousand electron volts per center.

Evidently, as mentioned above, there are two sources of vacancies in the lattice: The first requires little energy to produce a free vacancy, but can produce only a limited number of vacancies. The second produces many more vacancies, but at a greater expenditure of energy per vacancy. Because of the high efficiency and early exhaustion, the first source is generally identified with the vacancies initially present in the lattice. For

---

* Research supported by a U. S. Atomic Energy Commission contract.

† Submitted by one of the authors (P.V.M.) in partial fulfillment of the requirements for the degree of Doctor of Philosophy at the Carnegie Institute of Technology, June, 1960.

‡ Now at Westinghouse Electric Corporation, Atomic Power Department.

§ Present address: Princeton University, Princeton, New Jersey.

[1] I. Estermann, W. J. Leivo, and O. Stern, Phys. Rev. **75**, 627 (1949).

[2] K. Sakaguchi and T. Suita, Technol. Repts. Osaka University **2**, 177 (1952).

[3] I. L. Mador, R. F. Wallis, M. C. Williams, and R. C. Herman, Phys. Rev. **96**, 617 (1954).

[4] R. B. Gordon and A. S. Nowick, Phys. Rev. **101**, 977 (1956).

[5] B. Mozer and P. Levy (private communication, 1956).

[6] H. W. Etzel and J. G. Allard, Phys. Rev. Letters **2**, 452 (1959).

[7] P. V. Mitchell, D. A. Wiegand, and R. Smoluchowski, Phys. Rev. **117**, 442 (1960).

[8] P. V. Mitchell, thesis, Carnegie Institute of Technology, 1960 (unpublished).

the opposite reasons, the second source is associated with the production of new vacancies. At low temperatures the growth curve does not have a rapid rise in the early part but is linear (Fig. 2) from the start until saturation sets in, indicating that the first source, for some reason, is inoperative or greatly suppressed. This suggests that the vacancies initially in the lattice are bound to impurities or vacancy clusters and may be liberated by x rays only with the assistance of thermal energy. A further discussion of this point is given later on.

Other evidence for the existence of two processes comes from the bleaching of *F* centers. A bleaching curve cannot be fitted by a simple decay curve,[9] but requires at least two decay constants, suggesting that all the *F* centers may not be in the same environment. In addition, the magnitude of the decay constants at low temperatures[10] indicates that the color centers must be much closer together than they would be if they were randomly placed in the crystal. Most of the centers appear to be located in small regions with a high local density of centers, perhaps as high as 10^{20} cm^{-3}. This is supported by the measurements of conductivity in NaCl by Ingham,[11] from which one may conclude that only about one percent of the volume of a crystal contains most of the vacancies.

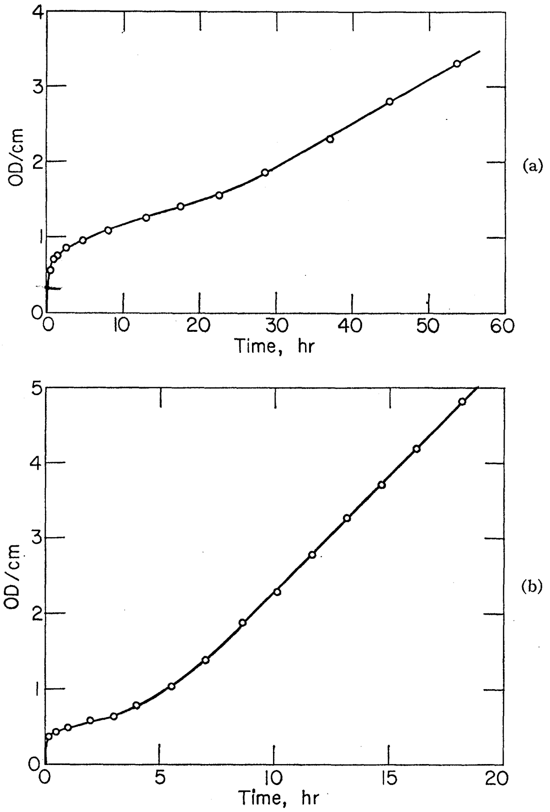

FIG. 1. (a) A growth curve of *F* centers in KCl at room temperature irradiated with 45 kv, 4.5 ma, through 0.02 mm Cu. (b) A growth curve of *F* centers in KCl at room temperature irradiated with 0.245×10^6 r/hr of Co^{60} γ rays (Mozer and Levy).

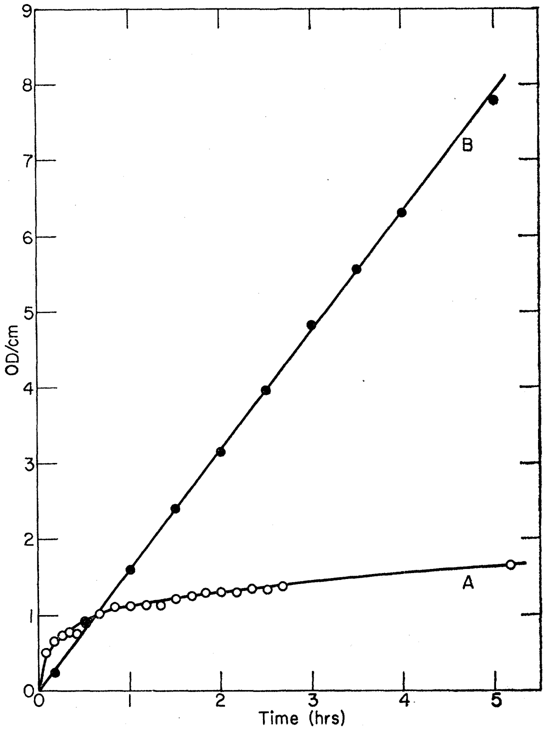

FIG. 2. *F*-center growth curves in KCl. Curve *A*—room temperature; Curve *B*—liquid nitrogen temperature.

1. Formation of F centers from Initial Vacancies

The rate of growth of *F* centers from initial vacancies by electron capture will be proportional to the number of vacancies available for coloration. If one also considers an annealing that is proportional to the number of centers present, then one obtains

$$df_i/dt=bn_i-\alpha f_i \quad (f_i=0 \text{ at } t=0) \qquad (1)$$

where f_i is the density of *F* centers, α is a bleaching constant, b is the rate constant for electron capture per vacancy, and n_i is the density of free vacancies that have been released from clusters but not yet filled with electrons. The rate of growth of n_i is equal to the rate at which free vacancies are released from clusters less the rate at which free vacancies are converted to *F* centers by electron capture. Thus, if n_0 is the initial density of vacancies in the crystal and γ is the rate constant for release, then

$$dn_i/dt=\gamma[n_0-(n_i+f_i)]-df_i/dt \quad (n_i=0 \text{ at } t=0)$$

---

[9] E. E. Schneider, *Fundamental Mechanisms of Photographic Sensitivity* (Butterworths Scientific Publications Ltd., London, 1951).

[10] J. J. Markham, R. T. Platt, and I. L. Mador, Phys. Rev. **92**, 597 (1953).

[11] H. S. Ingham, Jr., thesis, Carnegie Institute of Technology, 1958 (unpublished); H. S. Ingham, Jr., and R. Smoluchowski, Phys. Rev. **117**, 1207 (1960).

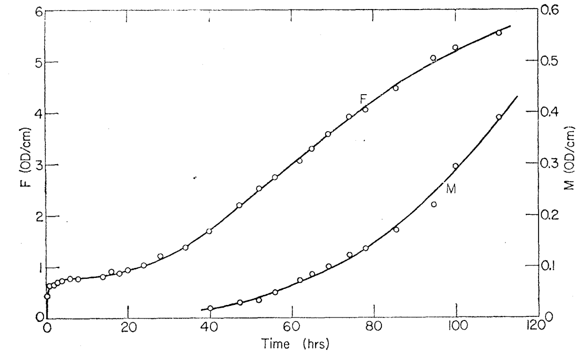

FIG. 3. Growth curves of F and M centers in KCl (Sample $H4$).

or

$$d(n_i+f_i)/dt=\gamma[n_0-(n_i+f_i)], \tag{2}$$

which has the solution

$$n_i+f_i=n_0(1-e^{-\gamma t}).$$

One thus obtains

$$df_i/dt=b[n_0(1-e^{-\gamma t})-f_i]-\alpha f_i, \tag{3}$$

which leads to

$$f_i=bn_0\left[\frac{1-e^{-(b+\alpha)t}}{b+\alpha}-\frac{e^{-\gamma t}-e^{-(b+\alpha)t}}{b+\alpha-\gamma}\right]. \tag{4}$$

There are two limiting cases of interest: Case I: $\gamma \gg (b+\alpha)$, Eq. (4) then reduces to

$$f_i\cong\frac{bn_0}{b+\alpha}[1-e^{-(b+\alpha)t}]=n^*(1-e^{-b^*t}), \tag{4a}$$

where $n^*=bn_0/(b+\alpha)$ and $b^*=b+\alpha$. This is a simple saturation curve. It should be noted that the product $b^*n^*=bn_0$ is independent of the bleaching rate α and its dependence on intensity of irradiation should be through b alone. Case II: $\gamma \ll (b+\alpha)$, Eq. (4) then reduces to

$$f_i=\frac{bn_0}{b+\alpha}[1-e^{-\gamma t}]=n^*[1-e^{-\gamma t}]. \tag{4b}$$

This curve has the same shape and saturation value as the one in case I, differing only in the time constant.

2. *Growth of F centers from Generated Vacancies*

The rate of growth of F centers from generated vacancies by electron capture will be proportional to the number of free vacancies that have been generated but not filled with electrons. That is,

$$df_g/dt=cn_g-\beta f_g \quad (f_g=0 \text{ at } t=0) \tag{5}$$

where f_g is the density of color centers, c is the rate at which a vacancy captures electrons, n_g is the density of free vacancies, and β is a bleaching constant. The growth of n_g is governed by the rate at which vacancies are produced and the rate of their transformation into F centers. If a is the rate of production of new vacancies, then

$$dn_g/dt=a-df_g/dt \quad (n_g=0 \text{ at } t=0) \tag{6}$$

or

$$d(n_g+f_g)/dt=a,$$

which gives $n_g+f_g=at$. Substituting into (5), we find

$$df_g/dt=c(at-f_g)-\beta f_g, \tag{7}$$

with the solution

$$f_g=\frac{c}{c+\beta}at-\frac{ca}{(c+\beta)^2}[1-e^{-(c+\beta)t}]$$
$$=a^*t-\frac{a^*}{c^*}(1-e^{-c^*t}), \tag{8}$$

where $a^*=c/(c+\beta)a$ and $c^*=c+\beta$. Note that $ac=a^*c^*$ is independent of the bleaching constant β.

In this derivation the rate of generation of vacancies, a has been assumed to be constant, which ignores the fact that eventually saturation does occur. The results of the derivation are thus certainly not applicable beyond the linear part of the growth curves. The onset of saturation, i.e., deviation from linearity could be due to many factors such as a back reaction or an exhaustion of the sources of generated vacancies or the formation of more complex centers at the expense of F centers. Figure 3 shows that in the beginning the

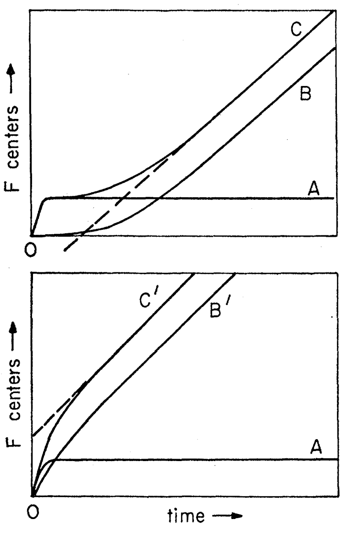

FIG. 4. Growth curves:
(A) $f_i=n^*[1-\exp(-b^*t)]$;
(B) $f_g=a^*t-(a^*/c^*)[1-\exp(-c^*t)]$;
(C) $f=n^*[1-\exp(-b^*t)]+a^*t-(a^*/c^*)[1-\exp(-c^*t)]$;
(B′) $f_g=a^*t-[(a^*/c^*)-n_0']\,[1-\exp(-c^*t)]$;
(C′) $f=n^*[1-\exp(-b^*t)]+a^*t-[(a^*/c^*)-n_0'][1-\exp(-c^*t)]$.

M band is weak and does not rise until the end of the linear part of the second stage of the *F*-center growth curve.

3. Discussion of the F-center Growth Curve

The measured density of *F* centers, f, is the sum of the contributions from each group of vacancies. Thus from Eqs. (4a), (4b), and (8):

$$f=f_i+f_g=n^*(1-e^{-b^*t})+a^*t-\frac{a^*}{c^*}(1-e^{-c^*t}), \quad (9)$$

where b^* is either $(b+\alpha)$ or γ, depending on whether one considers case I or case II. The general shape of the growth curve is shown in Fig. 4, where curve *A* is the contribution from the initial vacancies and curve *B* is the contribution from the generated vacancies. Curve *C*, the sum of *A* and *B*, i.e., the total density of centers, rises sharply to a plateau, goes through an inflection point, and then increases linearly with time. This is qualitatively the behavior that has been observed.[5–8]

In deriving Eq. (9) two tacit assumptions have been made: (1) It was assumed that vacancies were being converted only into *F* centers. This is not strictly true because vacancies may become bound as clusters and capture electrons, thereby forming directly more complex centers such as the *M* and *R* centers. It appears that the density of *F* centers to which Eq. (9) will be applied is in such a range that the complex centers are only a small fraction of those present. Actually the *M* band was the only complex band detected and it was small compared to the *F* band (Fig. 3). This is particularly true if the oscillator strength for *M* centers is 0.83 as recently indicated.[12] (2) It was also assumed that all of the vacancies initially in the lattice were uniformly distributed in small clusters. This is probably a good approximation for the crystals as they are received, but if the crystal has been deformed in some way the vacancies produced by plastic flow may be concentrated (either as single vacancies or as clusters) in small volumes of high local density. In this case one should add to Eq. (9) the term $n_0'(1-e^{c't})$ where n_0' is the initial density of these concentrated vacancies and c' is the rate constant for filling them with electrons. It will be shown later that these vacancies and those generated by irradiation both have high local densities and thus c' should be of the same order of magnitude as c^*. For discussion purposes, let us put $c'=c^*$ and lump this term with f_g. Then from Eq. (8)[13]:

$$f_g=a^*t-\left(\frac{a^*}{c^*}-n_0'\right)(1-e^{-c^*t}),$$

or

$$f=n^*(1-e^{-b^*t})+a^*t-\left(\frac{a^*}{c^*}-n_0'\right)(1-e^{-c^*t}). \quad (10)$$

Two interesting cases are: (a) $a^*/c^*>n_0'$ and (b) $a^*/c^*<n_0'$. In the first of these cases f_g and f have the same qualitative behavior as was discussed above. However, the plateau would not be as evident and the inflection point might not be noticed. In the second case, the shapes of f_g and f are altered. Figure 4 shows f_i, f_g, and f, labelled *A*, *B*′, and *C*′, respectively, for this case. The growth curve does not have an inflection point and the time constant for the initial rise will be c^* if $n_0'\gg n^*$. On this basis one would then expect the growth curve of a crystal deformed prior to irradiation, i.e., with nonrandomly distributed vacancies, to have a time constant for the initial rise which is longer than that of an undeformed crystal. The same effect would be noticed if the radiation intensity was such that $a^*/c^*<n_0'$ unless $n_0'\ll n^*$. If, on the other hand, vacancies were induced in a crystal by heat treatment, they would be fairly randomly distributed. The growth curve should then have a higher plateau but the same time constant for the initial rise when compared to the growth curve of an untreated crystal.

B. Rate of Electron Capture by Vacancies

The rate of electron capture per vacancy is $\phi\sigma$, where ϕ is the flux of electrons in the conduction band expressed in electrons/cm²/sec and σ is the cross section for capture in cm². Since σ should be independent of x-ray intensity I, the dependence of $\phi\sigma$ on intensity is through ϕ, which is proportional to the density of electrons in the conduction band. The density of electrons is determined by the rate of production $(\sim I)$ and the rate of removal. One can then write for the net rate of production of conduction electrons

$$d\rho_e/dt=k_1I-\rho_e(k_2\rho_e+k_3\rho_v)=k_1I-k_2\rho_e^2-k_3\rho_v\rho_e, \quad (11)$$

where ρ_e is the density of electrons in the conduction band, ρ_v is the density of vacancies, and the k's are constants. It has been assumed here that electrons are removed by recombination with holes, presumably at some recombination centers, and that the density of holes is proportional to the density of electrons, giving a ρ_e^2 term. For a steady state condition we have two limiting cases which are of interest, case I: for $\rho_e/\rho_v\gg k_3/k_2$, $\rho_e=(k_1I/k_2)^{\frac{1}{2}}$ and case II: for $\rho_e/\rho_v\ll k_3/k_2$, $\rho_e=k_1I/k_3\rho_v$.

C. Creation of Vacancies by Irradiation

1. Varley Mechanism

Varley[14] suggested a possible mechanism for the generation of vacancies in alkali halides through the

---

[12] T. Tomiki, J. Phys. Soc. Japan **14**, 488 (1960).

[13] In reference 7 the authors used a four-parameter equation for the growth curve in as-received crystals. The new results on deformed crystals indicate the need of an additional parameter n_0'. While Eq. (10) has five adjustable parameters it appears that the order of magnitude of these parameters and their systematic variation with the history of the samples, deformation, heat treatment and irradiation intensity justifies assigning them a physical significance.

[14] J. H. O. Varley, Nature **174**, 886 (1954); J. Nuclear Energy **1**, 130 (1954).

multiple ionization of the halogen ion. When a halogen is multiply ionized, it finds itself at a position of high electrostatic energy. This position is unstable and a slight perturbation will cause the ion to move from its normal lattice site into an interstitial position. After recapturing all but one electron it becomes an interstitial halogen atom and can return to its normal site only with great difficulty, since its activation energy for diffusion may be about 2 ev.[15] In order for this mechanism to operate, the halogen must remain multiply ionized for a sufficient time for the expulsion to occur. The calculation of Howard and Smoluchowski[16] indicates that this condition may be satisfied, although Dexter's[17] estimate based on mobility of holes in an ideal band approximation leads to an opposite conclusion. Actually the distortion of the band structure in the proximity of a positive halogen ion is probably so large that the applicability of the ideal band model is questionable (see *Note added in proof* at the end of the paper). A direct estimate of the probability of an electron transfer from a negative to a neighboring positive halogen ion has not yet been made. Different lifetimes may be also be required by other mechanisms.[18]

If an incident photon produces multiple ionization by the Auger effect then the rate of creation of vacancies would be proportional to the intensity of irradiation. Varley's estimate of the efficiency of this process shows that it could account for the experimental rate of vacancy creation. If, however, double ionization is a two-step process then the constant a would be proportional to the square of the intensity of irradiation.

An estimate of the rate of two-step double ionization of halogen ions in an alkali halide can be made assuming: (a) that all x-ray energy absorbed in the crystal goes into ionization of halogen ions, and (b) that ionization occurs randomly on the various halogen ions without regard to whether or not they are already ionized. The latter is admittedly a very crude assumption. Let E be the energy per second per cm^3 absorbed by the crystal, τ be the lifetime of the singly ionized state (neutral halogen), and V be the energy required to produce a single ionization event. Then, on this model the rate of single ionization events is E/V per second per cm^3 and the equilibrium number of singly ionized halogen ions is $(E/V)\tau$ per cm^3. If n is the density of halogen ions in the crystal, the probability that a particular one is singly ionized is $E\tau/Vn$ and the probability that another ionization will occur on the same ion is E/Vn per second. The rate of double ionization of that particular ion is then the product $(E\tau/Vn)\times(E/Vn)=E^2\tau/V^2n^2$ per second. For the crystal as a whole the rate of double ionization per second per cubic centimeter is thus $E^2\tau/V^2n$.

For numerical evaluation the data of Mozer and Levy [Fig. 1(b)] will be used since the calculation of energy absorbed is easier for monoenergetic gamma rays than for a spectrum of x rays. An irradiation rate of 0.245×10^6 r/hr corresponds to an energy absorption rate of 4.61×10^{12} ev/sec/cm^3 in air or 7.07×10^{15} ev/sec/cm^3 in KCl. The density of chlorine ions in KCl is $n=1.5\times10^{22}$ cm^{-3} and $V\simeq10$ ev. Let us further assume $\tau=10^{-6}$ sec, which is the lower limit for τ if $\rho_e\leqslant10^{11}$ cm^{-3}.[12] The rate of double ionization becomes then $E^2\tau/V^2n=33$/sec/cm^3, while the slope of the linear part of Fig. 1(b) corresponds to 1.73×10^{12} centers/sec/cm^3. Obviously, the rate of double ionization calculated by this model is much too low to explain the experimental value, especially if τ were to be taken as low as 10^{-14} sec as suggested.[17]

2. *Dislocation-jog Mechanism*

A mechanism has been proposed by Seitz[19] and Markham[20] for the generation of vacancies in alkali halides by the evaporation of vacancies from jogs on dislocations. In this process an electron is trapped by the charge on a jog $(e/2)$. The total charge on the jog is then reversed $(-e/2)$ and it can trap a hole. The energy of recombination of the hole and electron is then available for ejection of a vacancy. If the hole and electron are each free, then, since the density of each is proportional to $I^{\frac{1}{2}}$ or I (Sec. II B), the rate of generation of vacancies will be proportional to I or I^2. If, on the other hand, the hole and electron are not free but are bound as an exciton then the rate of generation of vacancies should be proportional to the density of excitons. The density of excitons can be derived from $dN/dt=k_1I-k_2N$, where N is the density of excitons, I is the rate of irradiation, and the k's are constants. For a steady state condition one has $N=(k_1/k_2)I$, so that the density of excitons is proportional to intensity. For this model then the rate of generation of vacancies should be proportional to the intensity of irradiation.

If one assumes a density of dislocations of 10^5 lines/cm^2 and that one vacancy can be produced for each atomic position along the dislocation ($\sim10^7$/cm), then this process should saturate at about 10^{12} vacancies/cm^3 per jog. In order to reach the observed saturation level of about 10^{19} vacancies/cm^3, one has to assume either that there are of the order of 10^7 jogs/cm on the dislocations or else that new jogs are being formed.

III. EXPERIMENTAL

The KCl crystals were obtained from the Harshaw Chemical Company and measurements were made on as-cleaved, on deformed, and on heat-treated crystals. Irradiation was carried out with a tungsten anode

---

[15] R. D. Hatcher and G. J. Dienes, Bull. Am. Phys. Soc. **4**, 142 (1959).

[16] R. E. Howard and R. Smoluchowski, Phys. Rev. **116**, 314 (1959).

[17] D. L. Dexter, Phys. Rev. **118**, 934 (1960).

[18] C. C. Klick, Bull. Am. Phys. Soc. **5**, 185 (1960).

[19] F. Seitz, Phys. Rev. **80**, 239 (1950).

[20] J. J. Markham, Phys. Rev. **88**, 500 (1952).

TABLE I. Results of curve fitting.

Sample number	Intensity (R/hr)	Thickness (mm)	a^*(OD/cm/hr)[a]	b^*(hr^{-1})	c^*(hr^{-1})	n^*(OD/cm)	n_0'(OD/cm)	Treatment
I 1	300	1.45	0.00276	(0.566)	0.0527	0.280	0.467	As cleaved
I 2	1 200	1.38	0.00245	1.23	0.106	0.337	0.246	As cleaved
I 3	2 700	1.05	0.00546	1.23	0.104	0.66	0.225	As cleaved
I 4	4 800	1.03	0.00914	1.58	0.041	0.783	0.718	As cleaved
I 5	14 700	0.85	0.184	2.15	0.088	0.998	0.0143	As cleaved
I 6	30 000	0.75	0.308	(3.74)	0.130	(1.63)	(2.93)	As cleaved
I 7	7 500	1.22	0.00775	2.08	0.084	1.085	0.394	As cleaved
I 8	10 800	1.24	0.0957	2.01	0.0416	0.957	0.536	As cleaved
I 9	14 700	1.58	0.121	1.85	0.071	1.26	0.253	As cleaved
I 10	19 200	1.59	0.266	2.43	0.070	1.023	0.446	As cleaved
I 11	24 300	1.73	0.234	2.41	0.113	1.072	0.484	As cleaved
D 1	13 900	1.80	0.181	3.83	0.0487	0.716	0	As cleaved
D 2	13 900	1.74	0.103	2.84	0.0907	1.15	0.783	0.6% deformation
D 3	13 900	1.73	(0.057)	3.25	0.229	1.36	1.27	1.32% deformation
D 4	13 900	1.44	0.0858	3.68	0.355	1.14	1.22	1.56% deformation
D 5	13 900	1.23	0.0725	4.28	0.173	1.85	2.09	2.02% deformation
D 6	13 900	1.54	0.0686	2.03	0.156	1.94	2.42	3.04% deformation
H 4	11 500	2.00	0.127	5.88	0.0125	0.678	0	As cleaved
H 5	11 500	1.83	0.0045	1.97	0.0287	3.56	3.20	500°C, 10 hr, air quenched
H 6	11 500	1.55	0.080	4.67	0.0389	0.82	0	450°C, 10 hr, air quenched
H 7	11 500	1.55	0.104	6.09	0.0275	0.665	0	450°C, 10 hr, cooled 1°C/min
H 8	11 500	1.60	0.0711	4.25	0.0413	0.951	0.098	500°C, 10 hr, cooled 1°C/min

[a] OD is defined as $\log_{10}(I_0/I)$ where I_0 and I are the initial and the transmitted intensities.

x-ray tube, operating at 140 kvp and 5 ma. The beam was filtered through 4–6 mm of Al to remove soft x rays and assure body coloration. This is an important point since soft x rays produce surface effects and complicate the growth curves to such an extent that the inflection points are not discernible. The dose rate at the crystal position was measured by an r-meter and was in the range of 300 to 30 000 r per hour. Optical measurements were performed with a Beckman DU spectrophotometer and a Warren Spectracord recording attachment. The samples were kept in total darkness during the experiment. Plastically deformed crystals were compressed in a direction perpendicular to the direction of irradiation. Heat treatment of samples consisted of raising their temperature at approximately 1°C/min to a given temperature, holding at that temperature for several hours, and then either lowering to room temperature at approximately 1°C/min or "air quenching" by withdrawing them from the furnace and allowing them to cool quickly to room temperature.

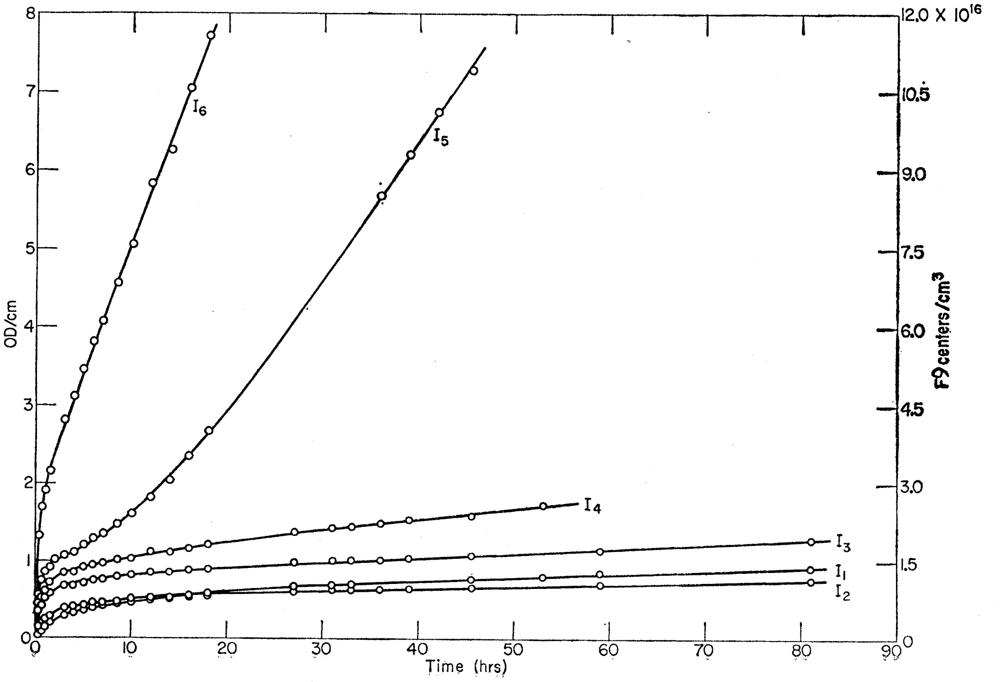

FIG. 5. Growth curves of *F* centers in Samples *I*1 to *I*6.

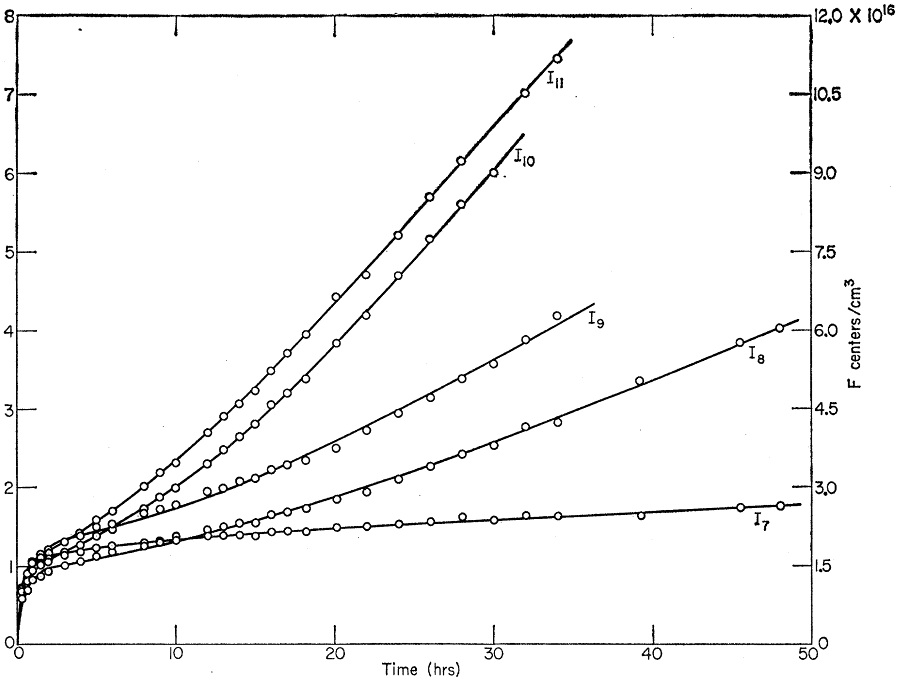

FIG. 6. Growth curves of *F* centers in Samples *I*7 to *I*11.

The physical treatment given each sample is shown in Table I. Further experimental details are given in reference 8.

IV. RESULTS AND DISCUSSION

1. *General*

The densities of color centers n_F and n_M were calculated from experimental data using Smakula's formula.[21] With the proper values for KCl at room temperature, one obtains $f_F n_F = 1.17\times10^{16}$ (OD/cm) for the *F* band and $f_M n_M = 3.3\times10^{15}$ (OD/cm) for the *M* band which leads to the approximate relations $n_F = 1.5\times10^{16} \times$(OD/cm) and $n_M = 5\times10^{16}\times$(OD/cm). The latter uses the lower limit for $f_M \cong 0.07$. This is pessimistic, since the more recent value of $f_M = 0.83$ would only emphasize that the *M* centers were negligible compared to the *F* centers.

It was found that the various parameters occurring in Eq. (10) could not be derived directly from the plots of n_F against time without excessive errors. Therefore a program was prepared to use an IBM 650 computer to fit Eq. (10) to the data by the least-squares method. Details of this program are given in reference 8. The experimental results are plotted in Figs. 5 to 8, the solid lines indicating the least-squares fits of Eq. (10) as determined by the parameters listed in Table I. The agreement is in general very good and covers a wide range of radiation intensities and various histories of the sample. It should be stressed again that in the derivation of Eq. (10) no attempt was made to include mechanisms leading to saturation and thus no consideration is given to growth curves beyond the linear part. It should also be pointed out that the general shape of the growth curve changes with the intensity of irradiation *I*. For low *I* the production of new vacancies is usually not observable for reasonable times of exposure. For high *I* the generation of new vacancies merges with the growth of *F* centers out of initial vacancies. Thus only in a restricted range of *I* can the plateau and the inflection point be observed. Further, the use of only hard, penetrating radiation which avoids high surface concentration of color centers as well as great precision in following the whole growth curve is necessary. Many of these precautions were not observed by other authors.

2. *Probable Errors*

It is of interest to consider now the physical interpretation, magnitude and variation of the various parameters appearing in the growth curve equation. The numerical values of the parameters given in Table I are those used in obtaining the various curves. As mentioned in reference 7, the computed curve fits the experimental points within an rms value of 2%. The probable errors of the parameters for a given curve are about 10%. There is more than 10% variation between parameters for samples which received similar irradiations because of difference in cleavage strains, purity, etc. This shows up in particular in the value of n_0' as expected. The quantity b^*n^* for samples *I*5, *I*9, and *D*1 is 2.12, 2.33, and 2.75, respectively, although these samples received essentially the same irradiation. This, we feel, reflects an inherent variation in the initial

---

[21] F. Seitz, *Modern Theory of Solids* (McGraw-Hill Book Company, Inc., New York, 1940), p. 664.

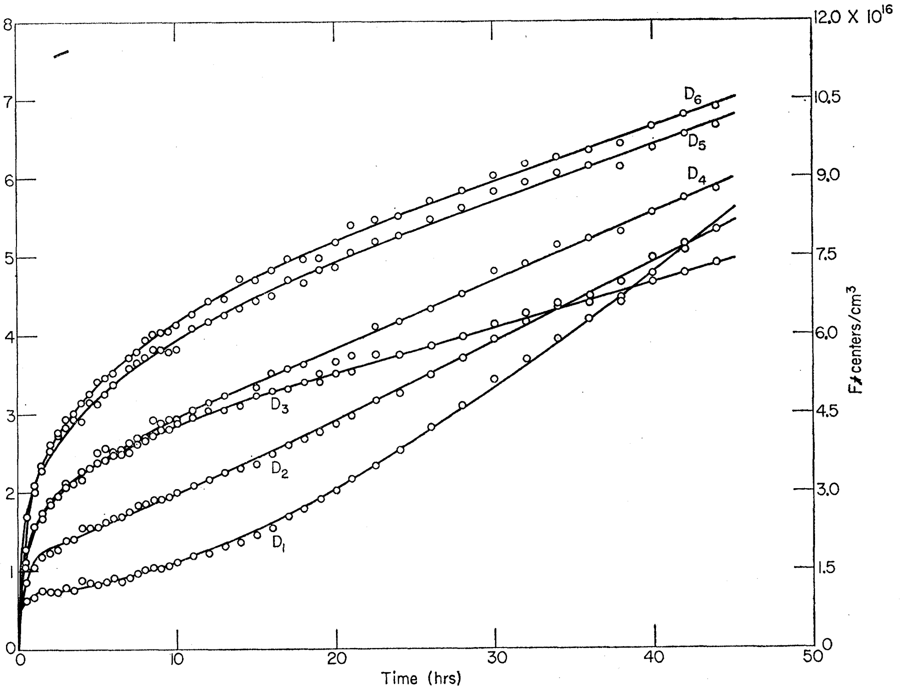

FIG. 7. Growth curves of *F* centers in Samples *D*1 to *D*6.

density of vacancies and is within the spread to be reasonably expected for "identical" samples of this material. Furthermore, the samples measured as a function of intensity and those measured as functions of deformation and heat treatment were cleaved from different batches.

The least reliable values are those for the low irradiation intensities, Samples *I*1 and *I*2, because of the large relative scatter of points. The probable errors for the parameters for these two samples are about 30%. The very low value of b^* for Sample *I*1 appears dubious and it is shown in Table I and in subsequent plots in parentheses. Similarly, in interpreting the parameters b^*, n^*, and n_0' for the Sample *I*6 one has to take into account the fact that the sample was considerably strained in cleaving which, as shown later, affects especially the parameter n_0'. The corresponding values are also enclosed in parentheses, both in Table I and in subsequent plots.

3. *Relation to Bleaching Experiments*

It is at this point heuristic to consider the bleaching experiments of Schneider[9] and Hesketh[22] since from their data it is possible to determine the observed ratio

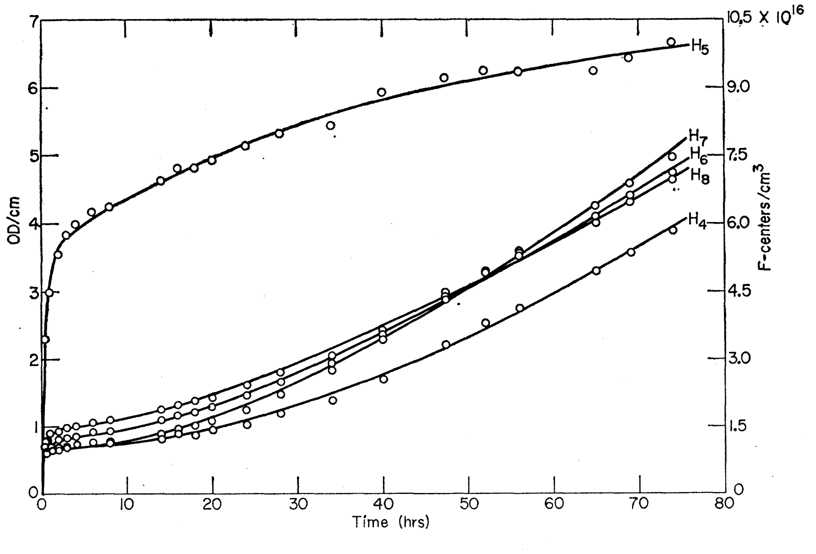

FIG. 8. Growth curves of *F* centers in Samples *H*4 to *H*8.

---

[22] R. V. Hesketh, Phil. Mag. 4, 114 (1959).

of c^* to b^* and the intensity dependence of these parameters. It will also be possible to make some deductions about differences in the local environment of the initial and the generated vacancies. Schneider has found that decay curves of F-center density in KCl under constant light illumination can be interpreted in terms of two bleaching rates for the centers. During the initial stages there is a rapid bleach which is independent of temperature. During this period no complex centers are formed. Following the rapid bleach there is a slow bleaching process which increases with temperature and during which other centers begin to appear on the long wavelength side of the F band. The quantum efficiency is unity for the rapid bleach and about 0.005 for the slow bleach. Referring to quantities introduced in Eq. (11) the quantum efficiency for bleaching, that is, the probability that an electron lost by an F center will recombine with a hole instead of being trapped by a vacancy, can be expressed by $q=k_2\rho_e/(k_2\rho_e+k_3\rho_v)$. In this form q depends on the incident radiation (for a given crystal) only through the electron density ρ_e. Applying this formalism to our experiments one can see that $q\cong 1$ requires $k_2\rho_e \gg k_3\rho_v$ which, applying Eq. (11) to a steady state, leads to $\rho_e=((k_1/k_2)I)^{\frac{1}{2}}$, where I is the x-ray intensity. Similarly, a quantum efficiency of 0.005 implies that $k_2\rho_e \ll k_3\rho_v$, giving

$$\rho_e'=k_1I/k_3\rho_v' \quad \text{and} \quad q'=k_2\rho_e'/k_3\rho_v', \tag{12}$$

(the quantities corresponding to low quantum efficiency are primed). Thus environments with low and with high vacancy densities should correspond to high and to low bleaching efficiencies, respectively. It is tacitly assumed that ρ_e during irradiation is such that the approximations leading to the two particular cases are applicable.

Hesketh analyzed color-center growth curves, using a different model, and also measured the quantum efficiency for bleaching as a function of the F-center concentration in KCl. He found that the latter is essentially unity up to about 2×10^{16} centers/cm^3 and then begins to decrease, reaching 0.1 at about 7×10^{16} centers/cm^3. Since 2×10^{16} centers/cm^3 is approximately equal to the concentration of initial vacancies in our crystals, it appears reasonable to associate the initial vacancies with the centers whose quantum efficiency would be unity and the generated vacancies with the centers whose quantum efficiency would be small. In terms of this model one would expect that the parameters b and c will be proportional to the local electron densities. We thus have

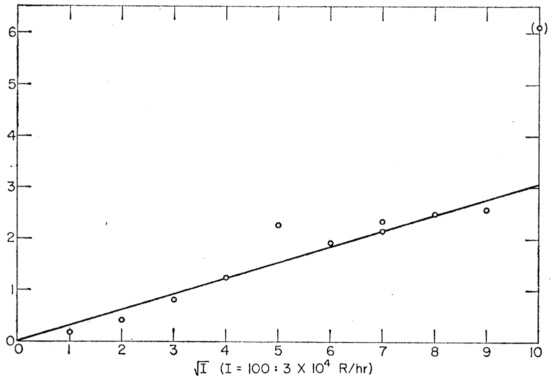

FIG. 9. b^*n^* vs $\sqrt{I}$ for Samples $I1$ to $I11$.

$$b=p\rho_e=p(k_1I/k_2)^{\frac{1}{2}} \quad \text{and} \quad c=p\rho_e'=pk_1I/k_3\rho_v', \tag{13}$$

where p is a proportionality constant and ρ_v' is the local density of generated vacancies. Combining (12) and (13), we have

$$\frac{c^2}{b^2}=\frac{k_2}{k_3\rho_v'}\,\frac{Ik_1}{k_3\rho_v'}=\frac{k_2\rho_e'}{k_3\rho_v'}=q'. \tag{14}$$

The ratio $c/b=(c^*-\beta)/(b^*-\alpha)$ varies considerably for various samples because of the large uncertainty in c^*. For the most reliable c^* values (see below) the ratio is 0.063 while the overall average is 0.050. These give for q the values 0.0025 and 0.0044, respectively, which are quite close to Schneider's value $q=0.005$. The small value of c relative to b appears to be due to competition among the generated vacancies for the limited number of electrons that are available in their vicinity.

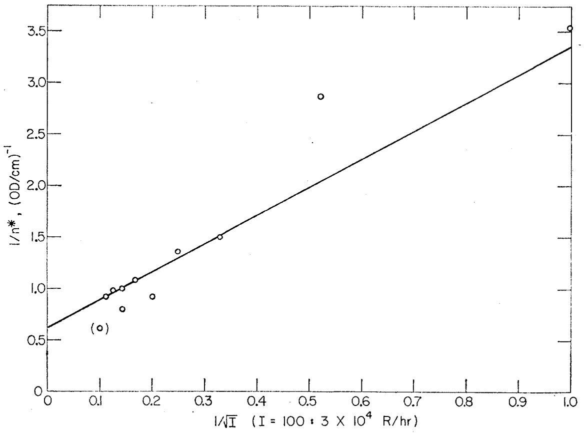

FIG. 10. $1/n^*$ vs $1/\sqrt{I}$ for Samples $I1$ to $I11$ (error for point at $I=4$ is 30%, see text).

Thus Schneider's results may be explained by associating the rapid bleach with the centers formed from the initial vacancies and the slow bleach with the centers formed from the generated vacancies. Initial vacancies are widely distributed and an electron ejected by a photon would have a very small chance of being recaptured by a vacancy before it recombined with a hole. This would give a quantum efficiency of unity. On the other hand, if the generated vacancies are concentrated in certain areas a liberated electron would have a high probability of being recaptured by a nearby vacancy with no net loss of F centers. A quantum efficiency of about 0.005 would mean that the average center must be excited 200 times before the electron is trapped by a hole. Since these F centers have a high local density it is not unreasonable that they should unite to form complexes as they are bleached. This would explain the growth of secondary centers as slow bleaching occurs.

4. Influence of Intensity of Irradiation

In the derivation of the growth curve it was found that $n_0^* = bn_0/(b+\alpha)$ and that $b^* = b+\alpha$ if $\gamma \gg (b+\alpha)$ or $b^* = \gamma$ if $\gamma \ll (b+\alpha)$. In the first case the initial growth rate is limited by the rate of electron capture by vacancies and in the second case it is limited by the rate of production of free vacancies from clusters. It is shown that it is reasonable to conclude from the data that in our experiments $\gamma \gg (b+\alpha)$ so that $b^* = b+\alpha$. A high value of γ also explains why the observed initial slope of the growth curve is usually quite high in spite of the implication of Eq. (3) that for $t=0$ it should vanish.

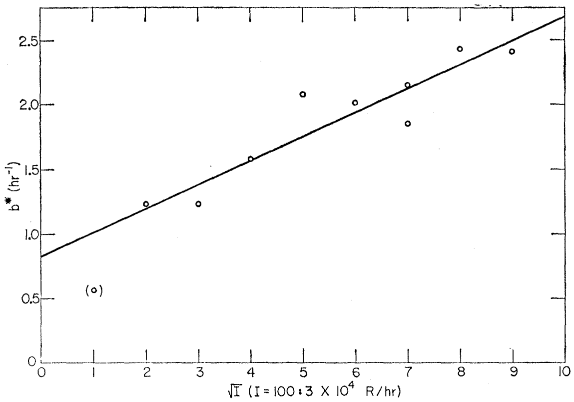

FIG. 11. b^* vs $\sqrt{I}$ for Samples $I1$ to $I11$ (a point of low accuracy for $I=100$ (i.e., for $\sqrt{I}=10$), see text, occurs at $b^*=3.74$).

As pointed out earlier, the product $b^*n^* = bn_0$ is independent of the bleaching constant α. A plot of b^*n^* vs $I^{\frac{1}{2}}$, shown in Fig. 9, is a straight line. This is in agreement with Eq. (13) which indicates that b should be proportional to $I^{\frac{1}{2}}$ and thus $b^*n^* = bn_0$ should also be proportional to $I^{\frac{1}{2}}$.

In order to estimate the parameters b, α, and n_0 the following relationship, for $b = kI^{\frac{1}{2}}$, can be used:

$$\frac{1}{n^*} = \frac{1}{n_0} + \frac{\alpha}{bn_0} = \frac{1}{n_0} + \frac{\alpha}{n_0 k I^{\frac{1}{2}}}.$$

The data are plotted in Fig. 10 in the form $1/n^*$ vs $I^{\frac{1}{2}}$ and within the limits of probable error, as discussed above, a straight line is obtained. Figures 9 and 10 give b, α, and n_0. To check the self-consistency of the data the following relationship can further be used:

$$b^* = b+\alpha = kI^{\frac{1}{2}} + \alpha,$$

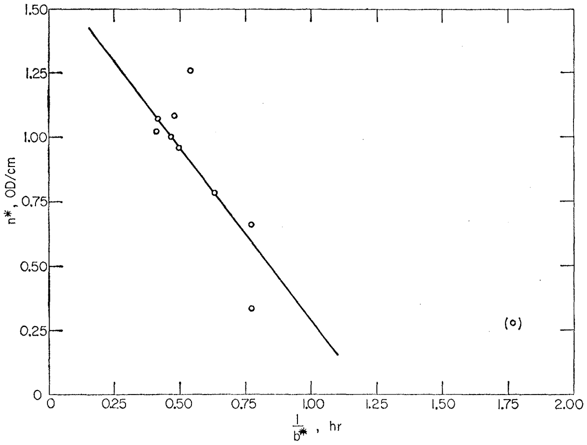

FIG. 12. n^* vs $1/b^*$ for Samples $I1$ to $I11$ (a point of low accuracy for $I=100$, see text, occurs at $n^*=1.63$, $1/b^*=0.376$).

and

$$n^* = \frac{bn_0}{b+\alpha} = n_0\left(1 - \frac{\alpha}{b^*}\right).$$

In Figs. 11 and 12 plots of b^* vs $I^{\frac{1}{2}}$ and n^* vs $1/b^*$ are given and again within the limits of probable error the relationships are found to be obeyed. In addition, the values of α, b, and n_0 obtained from Figs. 9 and 10 agree with the values deduced from Figs. 11 and 12. The best values are: $\alpha = 0.825$ hr^{-1}, $b = 0.185\ I^{\frac{1}{2}}$, and $n_0 = 1.62$ OD/cm $= 2.43 \times 10^{16}$ cm^{-3}. It should be pointed out that the constant α pertains to a bleaching process *during* irradiation only. There was no measurable bleaching occurring during the actual absorption measurements at room temperature.

The data indicate that α is essentially independent of intensity and that $b^* = b+\alpha$ rather than $b^* = \gamma$ except in the unlikely case that γ is proportional to $b+\alpha$. Curves calculated from the above values of α, b, and n_0 have been drawn on Fig. 13 through plots of the experimental values of b^* vs I and n^* vs I. c^* is also plotted for comparison with b^*.

The fast bleaching constants obtained by Schneider are roughly 1000 times as large as the slow bleaching

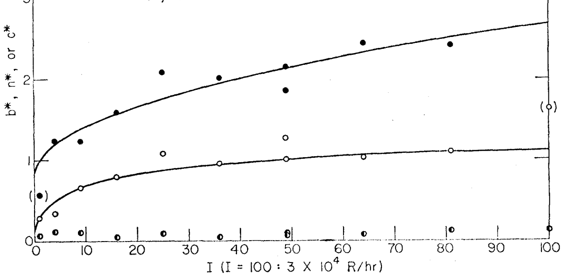

FIG. 13. b^*, c^*, n^* vs I for Samples $I1$ to $I11$.

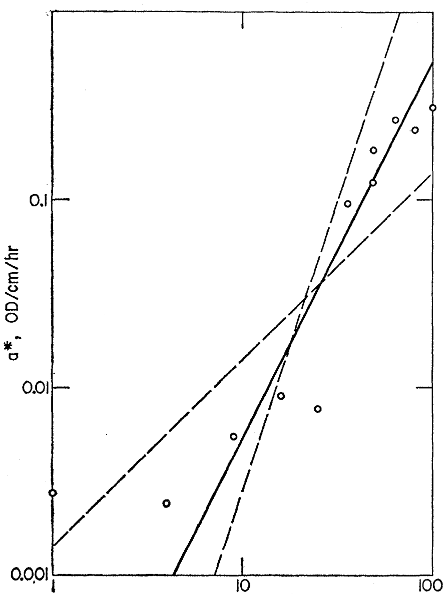

FIG. 14. a^* vs I for Samples $I1$ to $I11$ (point at $I=1$ has a 30% probable error, see text). The three lines have slopes 1, 2, and 3, respectively.

constants. Thus one would expect that $\beta \cong \alpha \times 10^{-3} \cong 0.001$. Since $c^* = c + \beta \cong 0.1$, β is negligible compared to c and thus $c^* \cong c$ and $a^* \cong a$. Figure 14, which is a log-log plot of a^* vs I, has a slope of two within the limits of experimental error, giving a^* a quadratic dependence on I. Its slope is definitely greater than one and less than three, as shown by the dotted lines. The scatter in these points may be due to deformation during cleaving since, as shown below, a^* is a strong function of plastic deformation. The scatter in c^* vs I (Fig. 13) is unfortunately so great that no conclusions can be drawn about the intensity dependence of c^*. The most accurate values of c^* are obtained from curves with a pronounced plateau such as $I5$ and $I9$ in Figs. 5 and 6. It is clear, however, that in all cases c^* is an order of magnitude smaller than b^*.

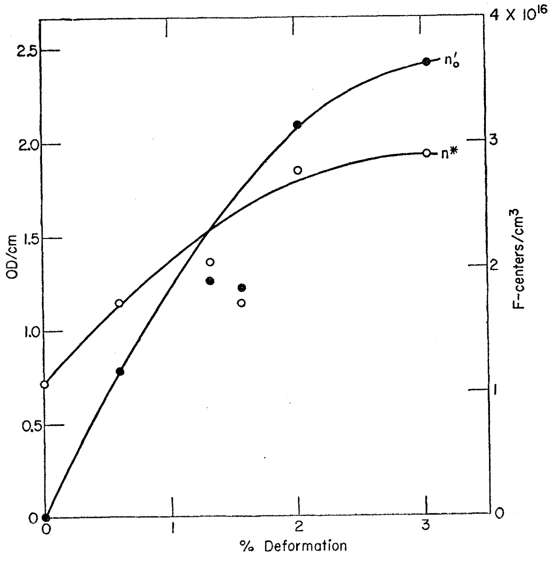

FIG. 15. n^* and n_0' vs % deformation for Samples $D1$ to $D6$.

5. *Influence of Plastic Deformation*

In plastically deformed crystals (Fig. 7) the initial density of vacancies was found to increase (Table I, Figs. 7 and 15). However, here the initial vacancies could be divided into two groups. In one group n^*, and thus n_0, varies slowly with deformation and the rate constants b^* are approximately equal to the rate constant of the initial vacancies in the undeformed sample. In the other group n_0' varies more rapidly with deformation and the rate constants c^* are comparable to the c^* of the undeformed sample. Apparently the main result of plastic deformation is to introduce additional vacancies in the wake of the moving dislocations. Most of these vacancies (n_0') remain in the region of high density but some vacancies move away, increasing n_0. One would expect that vacancies generated by plastic flow would be concentrated in certain regions of the crystal and the agreement between their rate constant and that of the vacancies generated by irradiation of the as-received crystal indicates that they have similar environments. This shows that the vacancies generated by irradiation are indeed localized.

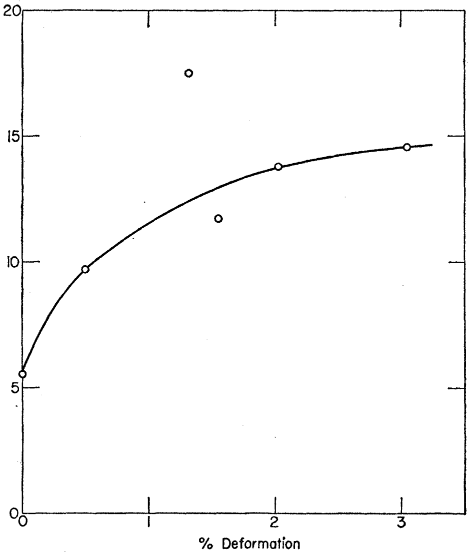

FIG. 16. $1/a^*$ vs % deformation for Samples $D1$ to $D6$.

Another interesting result of the measurements on deformed crystals is the decrease in the rate of generation of vacancies (a^*) with increasing deformation (Table I, Figs. 7 and 16). Since deformation presumably increases the density of dislocations and of jogs it is difficult to reconcile this observation with either the Varley or dislocation-jog mechanisms. A similar result has been obtained by Rabin.[23] He measured the rates of expansion of NaCl crystals from different sources and with various impurity concentrations. The natural crystal had the lowest rate of expansion although under polarized light it appeared to be highly strained and etch pit counts indicated a dislocation density higher than the other crystals.

The influence of deformation on coloration should be particularly pronounced when multiple slip sets in and the rate of generation of vacancies is greatly accelerated.[24]

6. *Influence of Heat Treatment*

Samples $H4$ to $H8$, as shown in Table I, indicate the influence of heat treatment. It was found that quenching from a particular temperature increases the initial density of vacancies n^* relative to the slowly cooled sample and that this effect is greater at the higher temperature. A quenching from 500°C, for example, increases n^* and thus n_0 by a factor of nearly five. This behavior is also easily seen in a qualitative manner in Fig. 8 where the time constant for the initial rise, i.e., essentially the parameter b^*, remains about the same but the total coloration goes up. In these experiments the cooling rate was rapid compared to that of the as-received crystals and thus the results are reasonable. What is important to note is that the rate constant for electron capture by the additional vacancies was essentially that of the initial vacancies in the as-received sample. This indicates that the initial vacancies and those induced by heat treatment have similar environments. Since the latter are most likely distributed throughout the volume, this indicates that the initial vacancies in the as-received crystals are also widely distributed. Sample $H5$ was apparently severely strained in quenching. This shows up in the large value of n_0' and in the lower slope of the linear part of the curve, low a^*.

Thus the deliberate introduction of known distributions of vacancies by heat treatment and by deformation provide additional evidence that the initial vacancies in the as-received crystal are well distributed and that the vacancies generated by irradiation are localized.

7. *Mechanism of Defect Formation*

It appears that there are several requirements that must be met by the mechanism of generation of vacancies by x rays in KCl at room temperature: (1) the interaction between the x-ray quanta and the ions must be through electronic excitation, (2) the vacancies must be generated in selected volumes of the crystal and with high local concentrations, (3) the mechanism must produce vacancies at a rate proportional to the square of the intensity of irradiation, and, finally, (4) an increase in dislocation density must reduce the rate of generation of vacancies. The Varley mechanism satisfies only the first and the third of these requirements but if it is a random second order process it is not very probable, as shown above. It could perhaps also satisfy the second requirement if presence of impurity centers was essential for its operation. The dislocation-jog mechanism satisfies most of the requirements but does not have the proper dependence on dislocation density. It appears thus that neither of these two mechanisms can be the dominant one at room temperature in KCl.

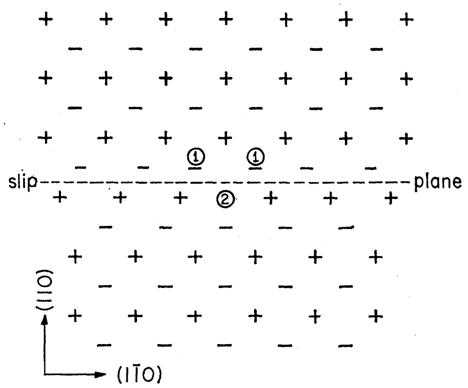

FIG. 17. Edge dislocation in an alkali halide crystal.

A new mechanism which retains certain features of the Varley and of the jog mechanisms is thus proposed. It satisfies all of the above requirements although, as pointed out below, it should be treated only as a preliminary model, requiring further experimental and theoretical confirmation. In any real crystal there are always some imperfections present which will alter the charge distribution, and therefore the electronic energy levels, in their vicinity. A positive-ion vacancy, for example, has an effective negative charge and thus reduces the binding of the $3p$ electrons in the neighboring halogen ions. These electrons then lie in localized energy levels above the filled band and should be more easily elevated to the conduction band than an electron in the filled band. Similarly, near the core of an edge dislocation in an alkali halide crystal there are halogen ions that do not have the proper number of nearest-neighbor alkali ions. These are labelled (1) in Fig. 17. Because of the missing positive ions, the ground state near these ions will lie above the valence band of the normal crystal. Besides, these ions are on the compression side of the slip plane and thus the forbidden energy gap is considerably narrowed. A rough estimate, based on the elastic approximation of the strain and on band calculations for NaCl,[25] indicates that this effect may be of the order of one ev. For both these reasons an exciton may provide enough energy to ionize one of

---

[23] H. Rabin, Phys. Rev. **116**, 1381 (1959).

[24] W. H. Vaughn, W. J. Leivo, and R. Smoluchowski, Phys. Rev. **110**, 652 (1958).

[25] J. C. Slater and W. Shockley, Phys. Rev. **50**, 705 (1936).

these halogen ions. The halogen atom, being neutral and much smaller than a halogen ion, can be pushed across the slip plane into the site, labelled (2), of highest tension, that is, opposite the edge of the dislocation. In this way both the compression strain and the tension strain are lowered. Although no specific calculations have been made this motion may be "down hill" all the way, i.e., without an activation energy. A second exciton decaying somewhere in the nearest neighborhood provides, in analogy to the jog mechanism, enough energy for a halogen ion from a normal lattice site to move into the vacancy left by the halogen atom. In this way the vacancy is permitted to escape the immediate edge of the dislocation. The halogen atom will soon recapture an electron and will occupy a normal halogen site along the edge of the dislocation. After a number of halogens have climbed onto the edge their charge will attract positive ions from the nearby lattice, thus creating positive ion vacancies and maintaining the neutrality of the dislocation in analogy to the jog mechanism. The net result of this process is the climb of the dislocation and the formation of highly concentrated negative and positive ion vacancies in the wake of the dislocation. Interstitials are not produced.

In Fig. 2 we have compared a low-temperature growth curve with a curve obtained at room temperature at the same low x-ray intensity. It appears that at low temperatures the process of generation of new vacancies is more effective. This may be due to a longer mean free path for excitons and a greater chance to decay at dislocations as suggested by the mechanism described above.

A detailed calculation of the efficiency of this process is very difficult but a rough estimate similar to that made for the normal Varley process can be made. Most of the excitons produced by x rays will decay at some recombination centers and traps. The distorted lattice and, in particular, the altered band structure on the compression side of dislocations, mentioned above, will provide very effective traps and centers for such a decay. It is thus reasonable to assume that a large part of the energy absorbed in the crystal will eventually be delivered to halogens in the cores of the dislocations. One then finds that the rate of the process is $E^2\tau/V^2n$ per cm^3 per sec, where n is now the density of halogen ions occupying these special sites and the other symbols are as previously defined. In a crystal with D dislocation lines per cm^2 and s special sites per cm of dislocation line, $n=Ds$. For the rate of double ionization one thus obtains $E^2\tau/V^2n=E^2\tau/V^2Ds$ sec^{-1} cm^{-3}. Inserting the same numerical data that were used above in the estimate of the Varley process and letting $s=10^7$ per cm and $D=10^5$ per cm^2 one obtains for the calculated rate of double ionization 5×10^{11} per sec per cm^3, which is a factor of 10^{10} higher than the corresponding value for the normal Varley process. In spite of the doubt as to the order of magnitude of τ it seems that the experimental rate of F-center formation 1.73×10^{12} centers/sec cm^3 definitely favors the mechanism here proposed. It should be borne in mind too that on the tension side of the slip plane the forbidden energy gap will be wider than normal and will, in effect, lower the concentration of electrons in the vicinity.[26] This may increase considerably the lifetime τ of the halogen atom as used in the above estimate. The mechanism clearly fits all the requirements imposed by the experimental data and it avoids the difficulties with producing a positive halogen ion and with the uncertain length of its lifetime.[17] At high temperatures the occurrence of the second excitation becomes less important and the rate of generation of new vacancies should be proportional to the intensity of irradiation.

It follows from the model that the more dislocations there are, the less chance there is that an ionization and a subsequent thermal spike will occur at essentially the same site along the dislocation network. This means that the rate of generation of vacancies given by this model should be inversely proportional to the dislocation density, that is, $a\propto1/D$. In addition, one might expect n_0', the number of vacancies produced by deformation, to be proportional to D^2 since these vacancies are produced by the intersection of pairs of dislocations. If this is so then $n_0'\sim1/a^{*2}$. A plot of n_0' vs $1/a^{*2}$ (Fig. 18) is indeed linear but does not pass

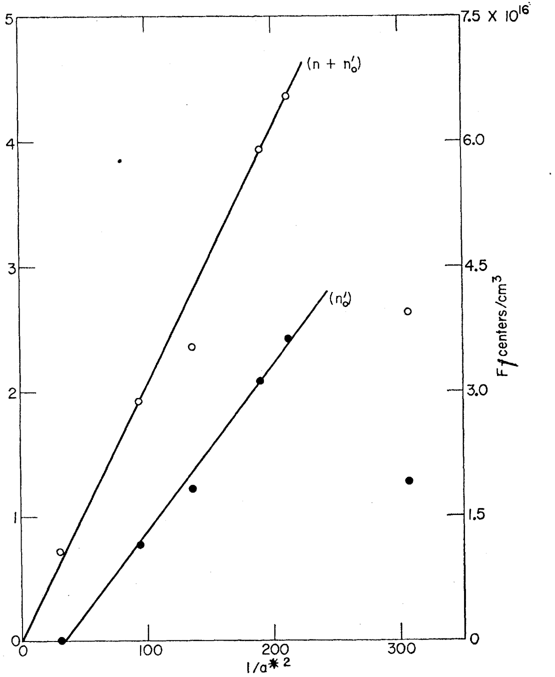

FIG. 18. n_0' and (n^*+n_0') vs $1/a^{*2}$ for Samples $D1$ to $D6$.

---

[26] J. A. Krumhansl (private communication).

through the origin as it should. On the other hand, a plot of the total number of vacancies initially in the lattice (n^*+n_0') vs $1/a^{*2}$ (Fig. 18) is also linear and passes through the origin. This suggests that the number of vacancies in the undeformed crystal is also related to the density of dislocations in the as-received crystal. This could be true if the density of initial vacancies were determined by equilibrium with the dislocations during crystal growth or if sufficient thermal strain were present during the cooling of the boule to cause the motion of dislocations and consequent generation of vacancies while the temperature was still high enough to homogenize the vacancies thus produced.

The requirements imposed by experiment are qualitatively fulfilled by another mechanism somewhat similar to the one proposed above: In this model two excitations lead to a double ionization of one of the ions, labelled (1) in Fig. 17, and this is followed by a displacement of the positive halogen ion onto the dislocation edge by the electrostatic repulsion of the positive metal ions. This mechanism suffers, however, from the uncertainties associated with double ionization and lifetime considerations. A similar situation occurs if the formation of positive halogen ions were to take place near impurities rather than at dislocations. Plastic deformation would lower the probability of double ionization by putting additional impurities into solution. One of the mechanisms of defect formation here proposed is probably applicable to the photolytic decomposition of potassium azide which shows a quadratic dependence on intensity of irradiation (see *Note added in proof* in reference 7).

It should be pointed out that the actual observed intensity dependence of a parameter, such as a, is a result of the intensity dependence of competing forward and back reactions of various relative importance. All one can say about the proposed model is that, for an intensity independent τ, it is consistent with the experimental results. It is not possible, at present, to estimate, even roughly, the relative importance of all the possible competing processes.

8. *Some Other Evidence for Two Kinds of F centers*

Two sets of other experiments indicate that there may be two kinds of *F* centers. There is evidence that indicates that the *F* band is not a simple absorption band. St. Petroff[27] and Konitzer and Markham[28] have found that as the *F* band is optically bleached the *M*, *N*, R_1, and R_2 bands grow, the peak of the *F* band shifts toward the violet, and the width at half-maximum of the *F* band increases. Thus there appear to be two *F* bands; the normal *F* band and a slightly displaced *F* band (designated as the *B* band by Petroff). The *B* band has a larger half-width and a higher maximum. The other experiment is that of van Doorn and Haven[29] who have found an apparent link between the *F* band and the *M* band. They irradiated a sample in the [100] direction with *F* light polarized in the [011] direction. This led to a growth of the *M* band when measured with light polarized in the [011] direction and to a bleaching of the *M* band when measured with light polarized in the [$0\bar{1}1$] direction. The opposite happens to the *F* band.

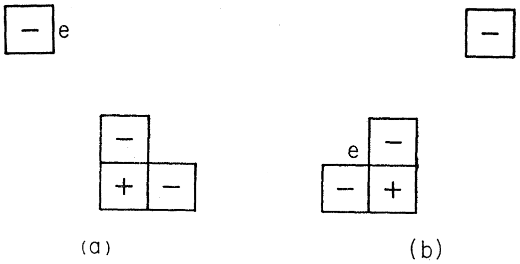

FIG. 19. Interaction between *F* and *M* centers.

These experiments can be interpreted in the following way. The *B* band is due to *F* centers whose vacancies have been generated by irradiation or by plastic deformation (perhaps induced by rapid quenching). Since these centers are located in regions of high local defect concentration they will be perturbed and give a band whose shape is slightly different from that of the isolated *F* centers. Among the debris in their vicinity will be complexes of positive and negative ion vacancies such as are associated with the *M* center. We shall consider two specific cases to illustrate the situation. First, let us take an *F* center situated in line with two negative ion vacancies of an *M*-center configuration, i.e., of an ionized *M* center [see Fig. 19(a)]. The empty vacancy cluster has a positive charge and will polarize the *F* center if the latter is not too far away. This configuration will be particularly sensitive to light with the electric vector along the line of the three negative-ion vacancies and thus an excitation and a transfer of the electron (perhaps by tunnelling) may occur. As a result, the concentration of a particular orientation of *M* centers will be enhanced and that of the corresponding *F* centers decreased. The other case occurs when an *M* center has in its vicinity a negative-ion vacancy situated in such a way that all the negative-ion vacancies are in line [Fig. 19(b)]. In this case the positive charge of the negative-ion vacancy will polarize the *M* center in such a way that the electron will spend more time in that vacancy of the *M* center which is nearest to the single negative-ion vacancy than in the other. This may lead to the formation of a polarized quasi-*F*-band of the *M* center. The configuration would thus be sensitive to an appropriately polarized *F* light and would lead to the transfer of the electron into the

---

[27] St. Petroff, Z. Physik **127**, 443 (1950).

[28] J. D. Konitzer and J. J. Markham, Phys. Rev. **107**, 685 (1957).

[29] C. Z. van Doorn and Y. Haven, Phys. Rev. **100**, 753 (1955).

single negative-ion vacancy. The concentration of the particular orientation of M centers would be decreased and of the corresponding polarized F centers increased. Clearly, there will be many other relative positions and orientations of vacancies and centers with appropriately higher or lower sensitivity to polarized F light. The model would also account for the more recent observations of Kawaba and Misu.[30] The above consideration is based upon the usual structure of M centers as proposed by Seitz and is equally applicable to its Knox[31] variant. If one accepts, however, the van Doorn model[32] then the argument may require considerable revision.

Nowick[33] has obtained results on NaCl that at first glance appear to be in disagreement with these results on KCl. To begin with, he did not observe an inflection point in the growth curve. The explanation lies probably in one of the reasons mentioned in the early part of the discussion of our results. Further, he found an increased colorability in the second stage due to deformation which he associated with a higher dislocation density. An examination of his growth curves shows, however, that the time constant for the initial rise is appreciably greater for the deformed crystals than for the as-received crystal. This is just what one would obtain if before irradiation the deformed crystals contained a mixture of both the random and locally concentrated vacancies so that the increased colorability is the result of the introduction of new vacancies by the motion of dislocations as proposed by Seitz and is in accord with our results. In other words, he observed a change in n_0' and not in a^*, which requires higher total irradiation. It should also be mentioned that during partial thermal bleaching the centers bleached first will be those formed from the vacancies n_0 that are randomly distributed. Upon re-irradiation, the time constant for recovery of coloration should be the same in both the early and later stages. It should, in fact, be equal to the time constant for the initial rise. Thus in the early stage of coloration the growth curve after partial thermal bleaching should parallel the curve before bleaching and in the later stage of coloration the growth curve after partial thermal bleaching should, after a time of the order of $1/b^*$, be an extension of the curve before bleaching. This effect is apparent in Nowick's data.

V. SUMMARY

A. The room temperature F-center growth curve for KCl has a form given by

$$f=n^*(1-e^{-b^*t})+a^*t-\left(\frac{a^*}{c^*}-n_0'\right)(1-e^{-c^*t}),$$

where the parameters are to be interpreted as follows:

(1) a^* is the rate of generation of new vacancies by irradiation; it appears to be proportional to the square of the intensity of irradiation and decreases with deformation, possibly as the inverse first power of the dislocation density.

(2) $n^*=bn_0/(b+\alpha)$ and $b^*=b+\alpha$, where n_0 is the initial concentration of randomly distributed vacancies, b is the rate of electron capture per vacancy, and α is a bleaching constant. As expected, b is proportional to the square root of the intensity of irradiation, α is independent of intensity, and n_0 is independent of intensity.

(3) n_0' is the average initial concentration of vacancies that are in small regions of high local concentration; it increases with deformation.

(4) c^* is the rate of electron capture per vacancy for the vacancies n_0' and for the vacancies generated by x rays.

B. The value of b^* is an order of magnitude greater than c^*. This, together with the behavior of n_0 and n_0' for deformed and heat-treated crystals, indicates that the vacancies generated by irradiation are localized in small regions with high local concentrations.

C. Both deformation and heat treatment strongly affect the growth curve. Heat treatment affects the early stage of coloration by increasing n_0. Deformation affects both stages of coloration by increasing n_0' and decreasing a^*.

D. Neither the Varley mechanism nor the dislocation-jog mechanism can be the dominant method of generation of vacancies by irradiation at room temperature. A mechanism has been proposed that appears to meet all the known requirements although it is not unique.

E. The proposal of Seitz that plastic deformation results in the generation of free vacancies through the motion of dislocations is verified.

Note added in proof. H. Fröhlich [Proc. Phys. Soc., London, **74**, 643 (1959) and private communication] has pointed out that the band approximation often breaks down when the carrier mobility is of the order of unity. This is just the case for the hole mobility in alkali halides (see reference 17).

---

[30] G. Kawaba and A. Misu, J. Phys. Soc. Japan **13**, 1038 (1958).

[31] R. S. Knox, Phys. Rev. Letters **2**, 87 (1959).

[32] C. Z. van Doorn, Phys. Rev. Letters **4**, 236 (1960).

[33] A. S. Nowick, Phys. Rev. **111**, 16 (1958).